



CELL-INTEGRATED SENSING FUNCTIONALITIES FOR SMART BATTERY SYSTEMS
WITH IMPROVED PERFORMANCE AND SAFETY

GA 957273

D4.3 – BMS-SLAVE—EQUIPPED BATTERY MODULE BASED ON THE
SERIES CONNECTION OF AT LEAST SIX 5AH PROTOTYPE POUCH CELLS
WITH LEVEL 1 SENSORS



Deliverable No.	D4.3	
Related WP	4	
Deliverable Title	BMS-slave—equipped battery module based on the series connection of at least six 5ah prototype pouch cells with level 1 sensors	
Deliverable Date	30-06-2023	
Deliverable Type	DEMONSTRATOR	
Dissemination level	Public (PU)	
Written By	Igor Pérez de Arenza (IKE) Joris de Hoog (FM) Glen Vandenbemt (FM) Lennert Es (FM)	15-06-2023 27-06-2023 27-06-2023 27-06-2023
Checked by	Joris de Hoog (FM)	06-07-2023
Reviewed by	Martin Wenger (FHG) Iñigo Gandiaga (IKE)	05-07-2023 29-06-2023
Approved by	Iñigo Gandiaga (IKE)	07-07-2023
Status	Final	07-07-2023



Summary

SENSIBAT This deliverable presents the progress made on the development of the battery module, incorporating all knowledge, technical work and insights of the SENSIBAT project. The main objective of task T4.3 is the development of a complete 24V module, consisting of 6 Level-1 SENSIBAT prototype cells. It includes the developed hardware (sensor readout, PMDU, BMS master and slave, external sensing, etc.).

The goal of the module is to validate the developed hardware and level-1 state estimation techniques, as well as to provide a platform to demonstrate all research and development performed during the project. Furthermore, we have developed a novel cooling block design, leveraging the presence of the thermal and pressure measurement points on the surface of the cells.

Due to the delay in the development and acquisition of certain parts necessary for the battery module's assembly, this deliverable is submitted with two-month delay compared to what is defined in the Annex I of the Grant Agreement (after Amendment approval). This document describes the design of the module and the included hardware. The delay in the design has a direct effect on the development of the battery module (Milestone 5). The whole SENSIBAT consortium is actively working to minimize the impact and mitigate any further delays. r task or activities within the project.



Table of Contents

1	Introduction	7
2	Module development	8
2.1	Requirements definition	8
2.2	Module Design.....	9
2.2.1	Main Module overview	9
2.2.2	Cell Stack overview	10
2.2.3	Sensors for verification of CFD	11
2.2.4	Sensors for verification of cell internal sensors.....	12
2.2.5	Plastic frames.....	12
2.2.6	Tension Rods.....	13
2.3	Cooling.....	13
2.3.1	Cooling architecture.....	13
2.3.2	Cooling Block design	14
2.3.3	Selection of cooling components.....	14
2.4	CFD analysis	16
2.4.1	CFD Objectives	16
2.4.2	Models and convergence analysis.....	16
2.4.3	Cooling Block design	17
2.4.4	Module thermal analysis	19
2.5	PMDU	22
2.5.1	Requirements.....	22
2.5.2	. ARCHITECTURE DESIGN	23
2.5.3	PCB Layout.....	23
2.6	BMS Master	24
2.7	BMS Slave.....	27
2.8	Sensor readout module.....	27
3	Discussion & Conclusion	29
3.1	Deviation in the delivery of milestone 5	29
4	Risks	30
5	Acknowledgement	31



List of Figures

Figure 1: Complete module testing unit, including the support structure and the battery module.....	9
Figure 2: Housing of the cell stack, showing the location of the main auxiliary hardware.....	10
Figure 3: Location of the cells, frames, thermal, pressure and flow sensors and the L1 sensor readout PCB.	10
Figure 4: concept of the battery stack.	11
Figure 5: Overview of the battery cell-stack design.....	11
Figure 6: Thermocouple at the centre of the pouch cell surface.....	12
Figure 7: Three load cells at one of the pressure plates.	12
Figure 8: Plastic frames inside the module stack. On the left side the functioning of the holes of the plastic frames is demonstrated, as the rod ensures correct position of the frame in the stack. On the right side the positioning of the cell in the centre of the stack is shown. Also, there are protruding tabs on the electrode side lowering the chance for accidental short-circuiting the cells with tools.	13
Figure 9: Flow reversal through use of 3-Way valves. On the left image, the cooled liquid enters the left side of the cooling blocks first. On the right image, the flow is reversed using the valves and the cooled liquid reaches the right side of the cooling blocks first.	14
Figure 10: Cooling block design with lid (left) and internal room for geometry (right).....	14
Figure 11: Cooling components from left to right: Alphacool VPP655 PWM pump (13195), Alphacool ES Flow and Temperature Indicator (17558), Aquacomputer G1/4 temperature sensor (53067).	15
Figure 12: BW3-034-AW1-R012DC 3-way Electrical Ball Valve.....	15
Figure 11: Comparison of series, parallel and pin-fin design.....	18
Figure 13: Temperature distribution over the cooling block.	18
Figure 12: Final pin-fin design.....	19
Figure 14: The temperature distribution of the module.	20
Figure 15: Average temperature comparison - steady VS flow switching.	20
Figure 16: Temperature steady comparison - steady VS flow switching.....	21
Figure 17: Pathlines and temperature distribution	21
Figure 18: Architecture Design – Main Block.....	23
Figure 19: 3D appearance of the assembled PCB.....	24
Figure 20: Battery management system architecture (hardware).....	25
Figure 21: BMS Master prototype.....	25
Figure 22: Graphical interface in LabVIEW	26
Figure 23: Graphical interface with SENSIBAT module Level 1 sensor data in LabVIEW.....	26
Figure 26: SENSIBAT BMS Slave PCB.	27
Figure 27: Block diagram of the stand-alone use case scenario of the read-out circuit. Source: D4.1	28
Figure 28: Read-out circuit PCB prototype	28

List of Tables

Table 1: List of module requirements.....	8
Table 2 - Simulation model comparison.....	16
Table 3 - Simulation base cell size analysis.....	17
Table 4: specifications of the PMDU.....	22
Table 5: PMDU interfaces.....	23
Table 6: specific thicknesses of the respective layers.....	24



Abbreviations

Symbol / Abbreviation	
AFE	Analog front-end
Ah	Ampere hour
ARD	Arduino
BMS	Battery management system
C-rate	Current referenced to battery capacity
CFD	Computational Fluid Dynamics
CNC	Computer Numerical Control
HMI	Human Machine Interface
HW	Hardware
IC	Integrated Circuit
L1	Level 1
L2	Level 2
NTC	Negative Temperature Coefficient
P	Pressure
PC	Personal Computer
PCB	Printed Circuit Board
PMDU	Power Measurement and Disconnection Unit
PWM	Pulse Width Modulation
RPI	Raspberry Pi
SLV	Slave
SoX	State of X (Charge/Health/Power/Safety)
T	temperature
V	Voltage
VAC	Variable Alternating Current
ZIF	Zero Insertion Force



1 Introduction

Within the SENSIBAT project, new 5Ah pouch cells have been developed in which temperature and pressure sensors in a 2D distributed grid have been integrated. The presence of these sensors allows us to measure both the temperature and pressure values of the total surface area of the cells. This information can be used for safety monitoring, condition monitoring, development of new state estimation techniques, understanding the location-dependent variations in temperature and pressure and so on.

To demonstrate these aspects to a wider audience, to test the scalability of the models and to validate these models, the SENSIBAT team has designed and is building an advanced battery module, in which 6 cells are connected in series to make a 24V module. During the design of the module, there were mechanical, thermal, electrical and safety aspects in constant consideration. The mechanical design is optimized for its intended function which is to be a demonstration and validation platform. To that end, the module is large and open, so that it stands self-supported on the floor, and is high enough for one to look inside as all components.

As the SENSIBAT Level-1 cells have an intricate grid of thermal and pressure sensors, an advanced cooling system has been designed to take advantage of this. The cooling concept has been discussed extensively and has undergone various iterations. Ultimately, a cooling block system with liquid cooling was chosen, as the cooling blocks also provide the needed preload to the cells. A novel reversible flow with asymmetric cooling blocks was chosen for the optimization of the surface temperature distribution.

Electrically, all cells must be connected in series in a safe and modular manner. For this, special separation brackets were 3D printed. The functioning of the cell is monitored by the Battery Management System (BMS), which is reading the input from all the L1-cell sensors via the BMS-slave, which in turn decodes the actual measurements from the sensor readout-PCB. A Power Measurement and Disconnection Unit (PMDU) monitors the current flow and can disconnect the module from the load when anomalies are detected. It is driven by the BMS-master.

Finally, the module has been equipped with many additional sensors for the validation of the internal L1-cell sensors and the state estimation algorithms.



2 Module development

2.1 Requirements definition

In this section, the requirements for the battery module demonstrator are explained. These requirements act as a guide when making design decisions.

Table 1: List of module requirements.

Functional
The demonstrator shall emulate relevant operating conditions with respect to the pouch cells <ul style="list-style-type: none">• Discharge rate (C-rate)• Environmental temperature• Thermal (cooling) interface The demonstrator shall visualize the data from the sensors in an interactive way <ul style="list-style-type: none">• Real-time display The demonstrator shall allow for verification of developed mathematical models <ul style="list-style-type: none">• CFD analysis: boundary conditions of model shall be measured by the demonstrator•• Coolant inlet/outlet temperature & flow rate•• Convective heat transfer with environment must be minimized, except for radiators The demonstrator shall allow for verification of developed sensing systems <ul style="list-style-type: none">• At least 1 calibrated external temperature sensor per cell to validate internal temperature sensors•• Temperature sensor shall be placed as close to cell surface as possible to increase accuracy• At least 1 calibrated external force sensor for the entire module to validate internal pressure sensors
Performance
Cooling should be optimized for uniform temperature distribution/minimal pumping losses <ul style="list-style-type: none">• Pump flow rate and thus pumping losses shall be adjustable for verification
Interfaces
Power: demonstrator shall be powered by single phase 220VAC outlet Thermal: demonstrator shall shed heat to environment through air cooling
Assembly
The demonstrator shall be non destructively disassemblable The demonstrator shall be modular The cell terminals shall be isolated from conductive components during assembly The demonstrator shall allow for measurement of pressure on the cells during assembly The coolant reservoir shall be at the highest point in the loop to avoid dry running the pump
Constraints
The demonstrator shall consist of 6 pouch cells connected in series Pouch cells will be identical and positioned in alternating order for easy series connection The module components shall be manufacturable using standard methods <ul style="list-style-type: none">• The cooling blocks shall be milled from aluminium using a 3-axis CNC machine•• Cooling block internal geometry shall have no space thinner than 4mm to avoid small milling cutters• Plastic components shall be laser-cut or 3D printed Demonstrator shall allow space for thermal/communication/power interfaces
Safety
Pouch cell terminals shall be electrically isolated from conductive components The demonstrator shall continuously keep the pouch cells within a safe temperature range <ul style="list-style-type: none">• 10°C to 40°C



2.2 Module Design

The complete module testing unit includes two parts, which are to be discussed separately:

- The actual module, housing the cells and performing the cooling.
- The support structure, housing the auxiliary electronics, radiators and additional measurement equipment.

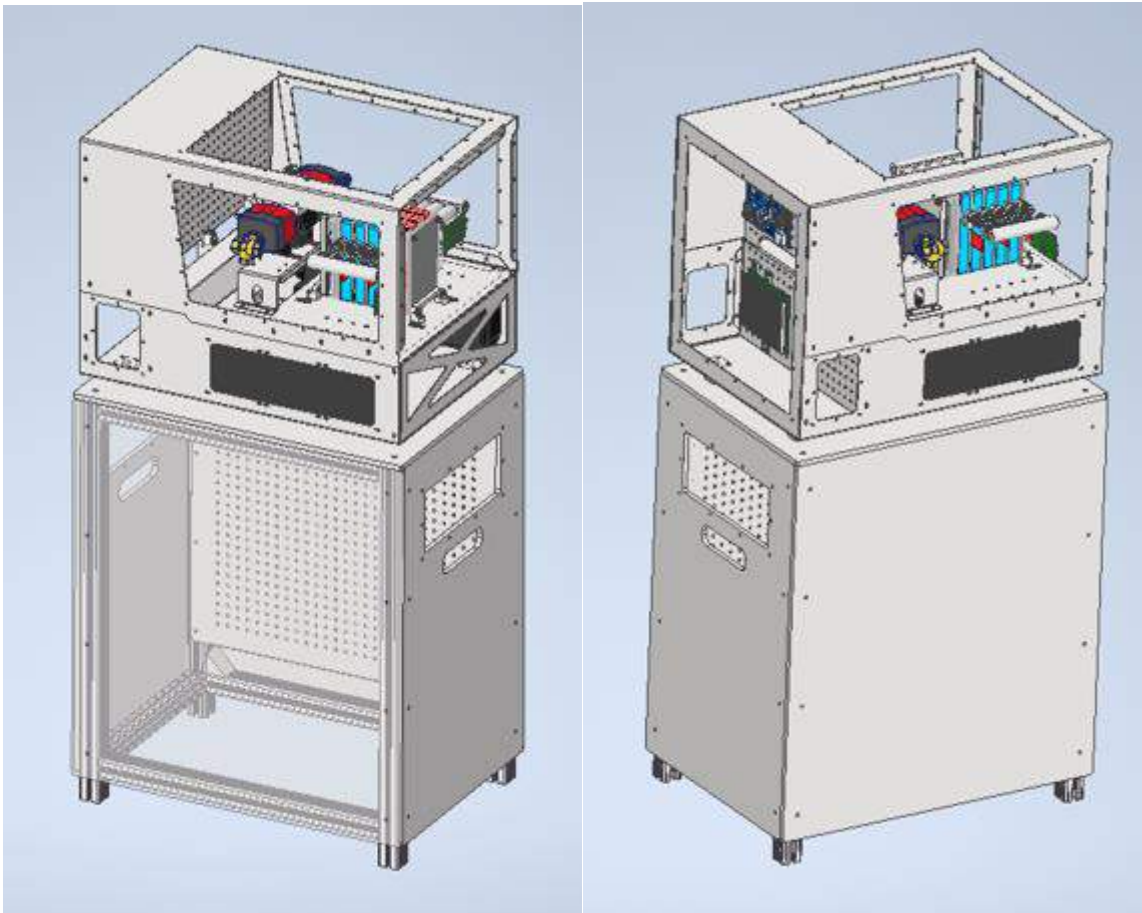


Figure 1: Complete module testing unit, including the support structure and the battery module.

Figure 1 shows the complete module testing unit. The cabinet on the bottom serves to house the auxiliary measurement equipment and is detachable from the upper unit. It will be fitted with wheels for easy transportation. The complete module testing unit is 1.3m high.

2.2.1 Main Module overview

The module which houses the cell stack, BMS master, BMS slave, PMDU and all cooling equipment is shown in Figure 2. It shows these items mounted on a vertical board where access to them is easy and quick.

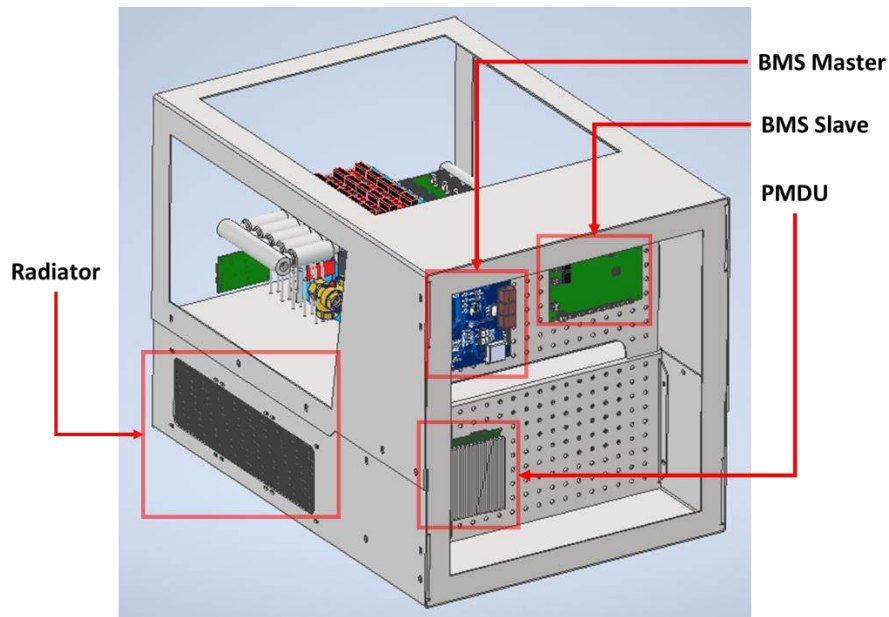


Figure 2: Housing of the cell stack, showing the location of the main auxiliary hardware.

The module housing the cells and all cooling equipment is shown in Figure 3. It shows the additional cooling related sensor equipment, the insulating plastic frames, the L1-cell sensor readout PCB and the 3 additional pressure sensors. All these items are presented below.

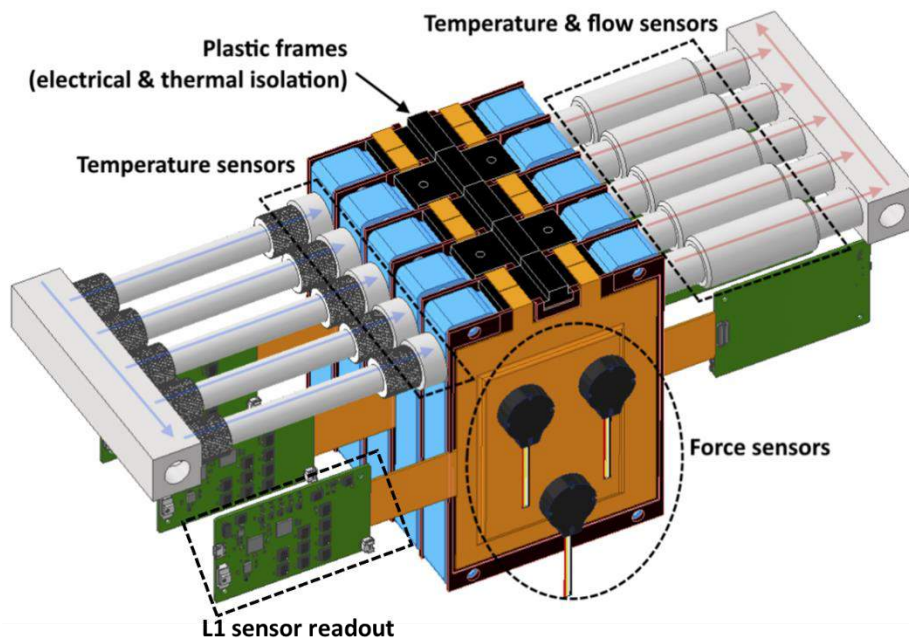


Figure 3: Location of the cells, frames, thermal, pressure and flow sensors and the L1 sensor readout PCB.

2.2.2 Cell Stack overview

The cell-stack consists of 6 SENSIBAT L1-5Ah battery cells connected in series with 5 cooling blocks in between (details of cooling block explained in section 2.3). The ends of the stack consist of insulated plates which allow a compression force to be exerted on the cell/cooling block stack (Figure 4).



Since the module consists of 5 cooling blocks, these requirements result in 5 coolant temperature sensors at one port and 5 combined flow rate/temperature sensors at the other port. Plastic frames provide thermal insulation around the cells to avoid unwanted convective heat transfer. See Figure 3 for reference.

2.2.4 Sensors for verification of cell internal sensors

As mentioned in the introduction and requirements (Section 2.1), the module should not only validate the mathematical models develop within the SENSIBAT project. Since the cells are fitted with SENSIBAT level 1 internal pressure and temperature sensors, this novel sensing approach must be validated as well.

For validation of the internal temperature sensors, each cell is fitted with a thermocouple in the centre of its outside surface. This will also allow to analyse the differential of having spatial temperature resolution and internal temperature.

For validation of the internal pressure sensors, one of the plates at the end of the cell stack is equipped with three load cell type force sensors. This allows not only for the verification of the total pressure on the cell stack, but also an estimate of the force distribution. For example, when tightening the tensioning bolts during assembly, the load cell readings will show when one side of the cell stack is clamped tighter than the other.

As can be seen, the external pressure sensors are placed against another aluminium plate, which is pressed against the rightmost cell. This plate is not threaded, meaning that the external pressure sensors will truly measure the change in pressure exerted by the cells during operation.

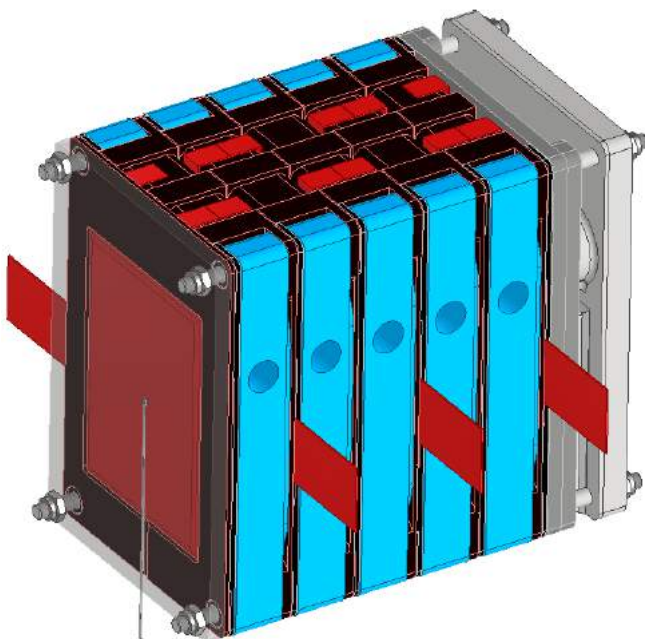


Figure 6: Thermocouple at the centre of the pouch cell surface.

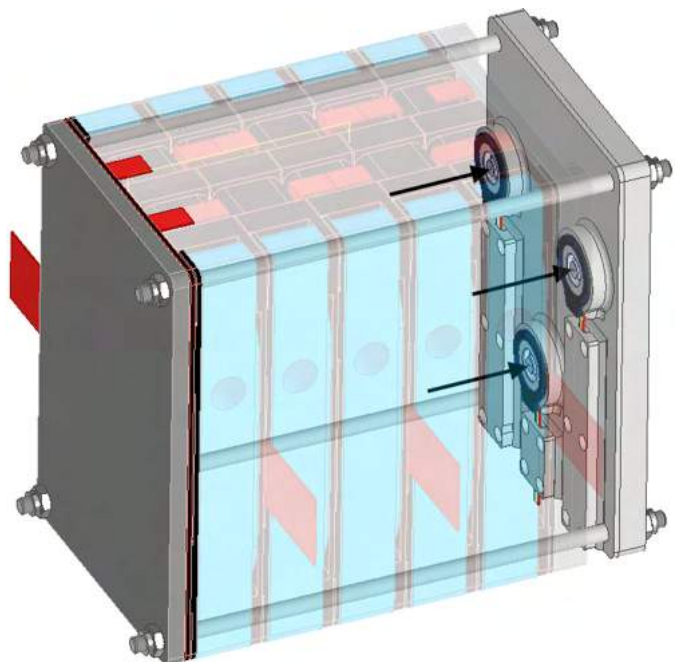


Figure 7: Three load cells at one of the pressure plates.

2.2.5 Plastic frames

The module stack contains 2 types of 3D printed plastic frames, these frames serve to satisfy multiple functions:

- XY-alignment of the pouch cells
- Thermal insulation of pouch cell perimeter to ambient air
- Electrical isolation of pouch cell terminals with metal cooling blocks
- Avoidance of shorting the terminals
- Reversible bolted connection of pouch cell terminals (no soldering/spot welding)

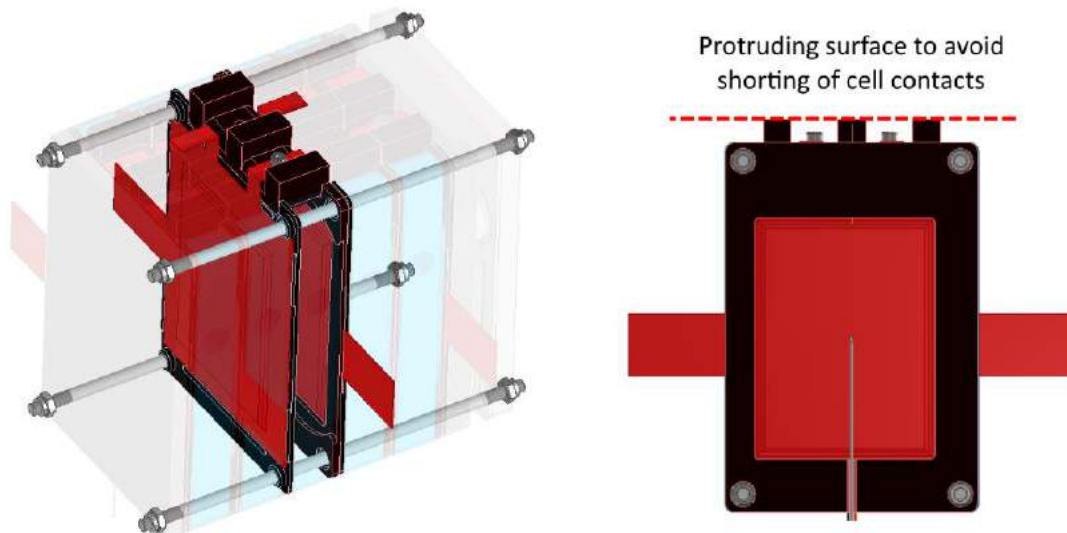


Figure 8: Plastic frames inside the module stack. On the left side the functioning of the holes of the plastic frames is demonstrated, as the rod ensures correct position of the frame in the stack. On the right side the positioning of the cell in the centre of the stack is shown. Also, there are protruding tabs on the electrode side lowering the chance for accidental short-circuiting the cells with tools.

These plastic frames are therefore a vital part of the module and greatly improve the flexibility of the complete cell testing module. The cell stack can be easily adapted to other cells of different chemistry, thickness, sensor application or other, simply by printing new versions of this plastic frame. As long as the cell surface dimensions are compatible with that of the cooling blocks and retaining plates, the cell stack can be adapted to it. This is an important feature for future project, in which one can reuse the cell stack without significant modifications.

2.2.6 Tension Rods

The tension rods that run throughout the module will be smooth rods with threaded ends as opposed to completely threaded rods. This is because the whole component stack will expand and contract during operation due to cell breathing and swelling. Fully threaded rods increase the chances of one of the components binding due to the threads grabbing the material.

2.3 Cooling

2.3.1 Cooling architecture

As briefly mentioned in the requirements (Section 2.1), the goal of the cooling approach is to achieve a uniform temperature distribution over the cell while minimizing the pumping losses. This can be achieved by high flow rates as this does not allow the coolant to heat up considerably. At lower flow rates to reduce pumping losses however, the coolant heats up considerably and the inlet temperature will be lower than the outlet temperature. A secondary goal is to have interactive visualization of the temperature data of the cells. To achieve a dynamic transient temperature distribution, keeping the cells in steady-state conditions is to be avoided. The combination of both requirements resulted in the concept of a cooling loop in which the direction of flow can be reversed (Figure 9). By switching the valves at regular intervals, the resulting temperature distribution will be more uniform than having the flow in a single direction due to the heat capacity of both the cell and cooling block walls. Since the requirements state that the cells must be cooled continuously, there is a radiator in the cooling loop to avoid excessive coolant temperatures.

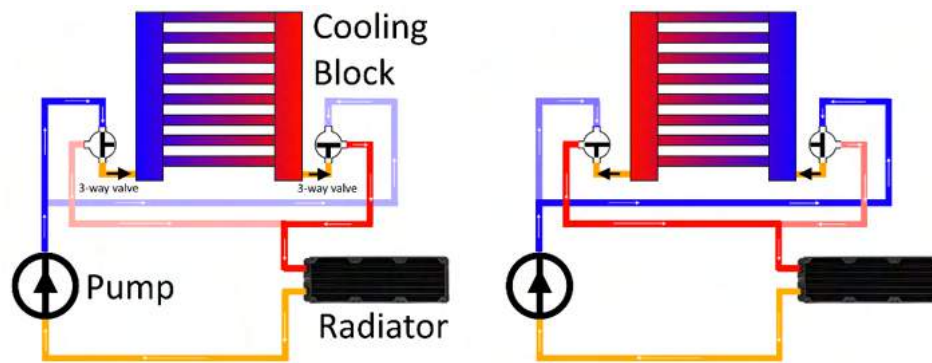


Figure 9: Flow reversal through use of 3-Way valves. On the left image, the cooled liquid enters the left side of the cooling blocks first. On the right image, the flow is reversed using the valves and the cooled liquid reaches the right side of the cooling blocks first.

2.3.2 Cooling Block design

2.3.2.1 Mechanical design

The cooling block will be made from aluminium due to its high thermal conductivity, ease of machining and relatively low cost. These cooling blocks will consist of an aluminium main body, sealing O-ring and aluminium cover plate. The length and geometry of the groove was dimensioned for internal pressure on an O-ring with 115mm inner diameter and 2mm thickness.

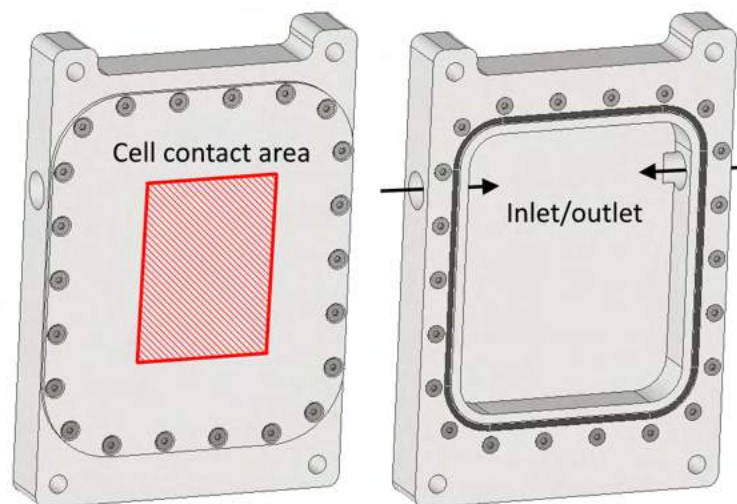


Figure 10: Cooling block design with lid (left) and internal room for geometry (right).

2.3.2.2 Cooling design constraints

The cooling block has been milled using a 3-Axis CNC mill due to cost considerations. This imposes constraints on the allowed geometry such as the geometry being 2.5D (meaning the CNC toolhead moves in layers, only on the XY-plane, like how a 3D extrusion printer works but with material subtraction instead of addition) with no internal channels smaller than 4 mm. Smaller internal channels would result in the use of very small milling cutters and long production times/costs.

2.3.3 Selection of cooling components

The cooling loop components were selected to be products manufactured for computers market (consumer electronics) water cooling components as these are mass produced and cheap, offer long lifespans and there is a whole ecosystem of compatible components.



2.3.3.1 Cooling pump

To assess the cooling effectiveness at multiple pumping losses/flow rates, the pump is required to be adjustable. During initial filling of the coolant loop, dry running of the pump is to be avoided to prevent damage. Due to these requirements, an adjustable flow rate (PWM signal) pump with built in reservoir was selected: Alphacool VPP655 PWM, see Figure 11.

2.3.3.2 Temperature and flow sensors

The temperature and flow sensors used in this project are the Alphacool ES flow and temperature indicator and the Aquacomputer G1/4 temperature sensor. The Alphacool sensor combines temperature and flow in one package and one is used per cooling block. The temperature sensor on the other side of the cooling block is then used to calculate the cooling efficiency of the cooling block. The selected components are primarily used in high-end cooling loops for personal computers and are rated for high load and continuous operation.



Figure 11: Cooling components from left to right: Alphacool VPP655 PWM pump (13195), Alphacool ES Flow and Temperature Indicator (17558), Aquacomputer G1/4 temperature sensor (53067).

2.3.3.3 Three way valves

As mentioned in section 2.3.1 the cooling loop will contain 3-way valves to allow for the reversal of flow direction. Since the goal of the design is to minimize (pumping) losses, the gains made should not be lost due to powering the valves. These valves should be of a type that only consumes power when switching from one state to the other. The chosen valve is of type BW3-034-AW1-R012DC. See Figure 12 for an image.



Figure 12: BW3-034-AW1-R012DC 3-way Electrical Ball Valve.



2.4 CFD analysis

2.4.1 CFD Objectives

A computational fluid dynamics (CFD) analysis will be performed during the design phase of the battery module. Ansys Fluent software will be used for these simulations. This will aid in designing a cooling block that strives for a uniform temperature distribution over the cell surfaces, a minimum pressure loss over the cooling blocks and maximum heat transfer from the cell.

The CFD analysis will also be performed after the battery module is operational. By comparing the real measurements from the module with the values from the CFD analysis, the model can be validated. If the model proves to be accurate it can be used for a more detailed analysis of the battery module without the need for additional complex measurement tools. This can aid in understanding the complexities of cooling a battery module and improve future cooling solutions.

2.4.2 Models and convergence analysis

2.4.2.1 Model

The choice of which CFD model to use is an important one. This refers to the numerical model by which the flow will be solved. A RANS-model was used in favour to more complex models like LES or DNS to save on computational time and cost.

The selection between the many different RANS-models that are available was made based on literature and a series of simulations on a very refined mesh with a geometry very comparable to the concluding cooling block. The main observables used in the simulations to determine convergence are the total heat transfer rate of the system, the average outlet temperature, the average battery temperature, the battery temperature standard deviation and the pressure drop over the cooling block. The generated mesh has a fine base cell size (0.15mm) so the model comparison is independent of mesh quality. Extra refinements were made where needed to reduce discretization of the geometry. The models analysed in the table below were selected because they are commonly used in industry. More information on these models can be found in the *Ansys Fluent Theory Guide*. The mesh was tested with, and without, boundary layers. When a boundary layer was used, a Y^+ of lower than 1 was ensured to completely resolve the boundary layer.

Table 2 - Simulation model comparison.

Model	Boundary layer mesh	Outlet avg temp (K)	Battery avg temp (K)	Battery stddev temp (K)	Pressure drop (Pa)
Laminar	yes	300.273	301.260	0.22	228.5
k- ω -SST	yes	300.268	301.200	0.19	222.8
k-kl- ω	yes	300.300	301.320	0.28	224.2
k- ϵ standard - enhanced wall functions	yes	300.307	301.373	0.18	188.0
k- ϵ RNG - enhanced wall functions	yes	300.302	301.296	0.18	188.4
k- ϵ realizable - enhanced wall functions	yes	300.306	301.371	0.18	187.7
Laminar	no	300.293	301.256	0.18	176.0
k- ω -SST	no	300.280	301.157	0.16	173.0
k-kl- ω	no	300.289	301.280	0.23	167.2
k- ϵ standard - standard wall functions	no	300.286	301.138	0.13	171.8



It was observed that the choice of simulation model or boundary layer did not have a large influence of the thermal characteristics of the simulation. However, it did have a significant impact on the pressure drop observed over the cooling block. The conclusion is that, if only thermal characteristics are of interest, a simple model like k- ϵ standard - standard wall functions is sufficient and will allow for fast calculation. If more complex flow phenomena are present, or if the pressure drop needs to be observed in detail, a more resolved model like k- ϵ realizable - enhanced wall functions and a mesh with an adequate boundary layer are needed. It was opted to use the k- ϵ realizable - enhanced wall functions since the pressure drop is of interest and because it is most suited to this application according to the *Ansys Fluent Theory Guide*. If great precision is desirable the models should be compared with the experimental data that will be obtained from the real battery module.

2.4.2.2 Convergence analysis

During the mesh convergence analysis, the base cell size of both the solids and fluids were analysed whilst using a fully resolved boundary layer mesh. Local refinements were always made so that the geometry was captured accurately and that no excessive gradients were present between neighbouring cells. The convergence analysis was performed with a geometry very comparable to the concluding cooling block.

Table 3 - Simulation base cell size analysis.

Base cell size (mm)	#Cells	Outlet temp (K)	avg Battery avg temp (K)	Battery temp (K)	stddev	Pressure drop (Pa)
2.5	130764	300.283	301.362	301.362	0.23	236.7
1.25	350118	300.282	301.286	301.286	0.22	226.1
0.625	1393847	300.291	301.284	301.284	0.22	221.7
0.3125	1733328	300.284	301.265	301.265	0.21	221.0
0.1563	7780553	300.281	301.261	301.261	0.21	220.1

Following the convergence analysis, it is concluded that for observation of thermal effects only a coarse mesh was required. A mesh with 50x more cells only resulted in a small difference of the observed values compared to the coarse mesh. However, if the flow effects of the fluid are to be observed, for example to capture recirculation or the pressure drop, it is advised to use a fine mesh with a fully resolved boundary layer. Based on these results it was opted to use a base cell size of 2.5 mm for the solid areas of the mesh and a base cell size of 0.625 mm for the fluid areas. Extra refinements were made where needed to fully capture the geometry. Other mesh variables were also observed during this convergence analysis, namely the boundary layer Y+ value, mesh conformality and element shape. These factors were found to have minimal impact on the observables of the simulation, hence, they will not be further elaborated upon.

2.4.3 Cooling Block design

For the design of the cooling blocks, multiple types of cooling channels were drawn based on common industry practices. Most of the designs fall into the serial, parallel or pin-fin channel design. Each cooling block was simulated using the same boundary conditions. Namely an inlet flow rate of 25 ml/s, and outlet pressure of 0 Pa gauge pressure, an incoming heat transfer rate of 20 W dissipated uniformly over the battery contact area (only on one side of the cooling block) and all other external surfaces were considered adiabatic. The different cooling blocks were then compared using the observed criteria, namely the average outlet temperature, the average battery temperature, the battery temperature standard deviation and the pressure drop over the cooling block.

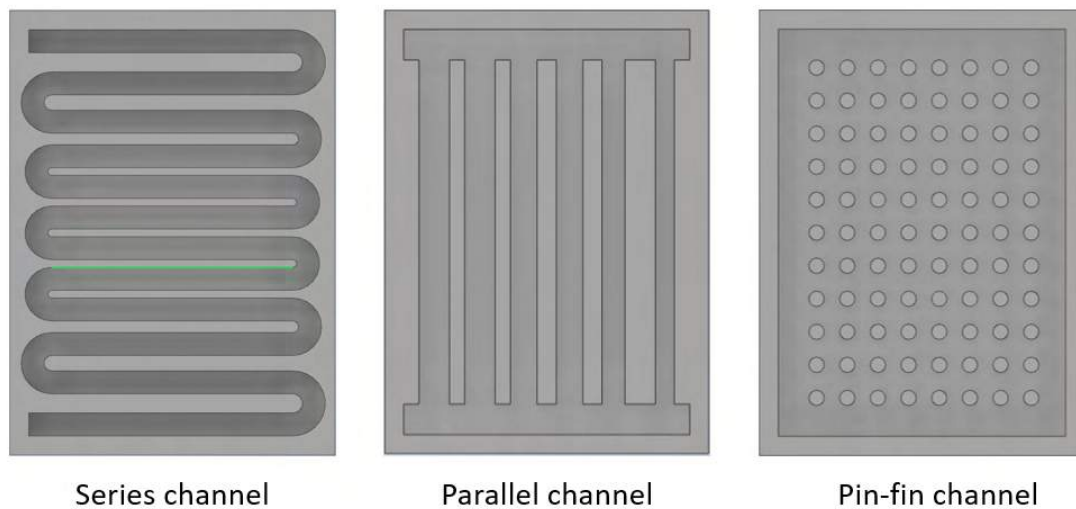


Figure 13: Comparison of series, parallel and pin-fin design.

Multiple iterations were made of all three types. The series channel had the lowest overall battery temperature, however it had the highest standard deviation of the battery temperature and a pressure drop around 5 times higher than the other designs. The parallel channel and pin-fin channel both performed admirably. However, optimizing the standard deviation of the battery temperature proved to be more convenient with the pin-fin channel. A few iterations were made to optimize the pin-fin design further and to take production constraints into account. In the picture below the final design is depicted along with the temperature distribution using a load case based on literature. For the final temperature distribution analysis, the load case will need to be adapted to the measured load of the cells used in the SENSIBAT project. Using experimental results of the SENSIBAT cells a new cooling block could be designed considering the correct heat transfer of the cells and using a non-uniform heat transfer distribution over the battery surface.

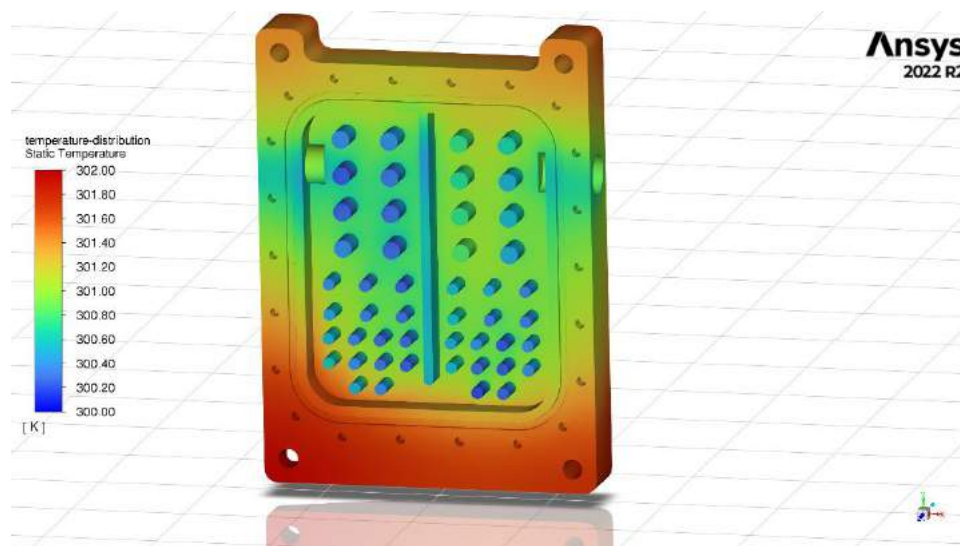


Figure 14: Temperature distribution over the cooling block.

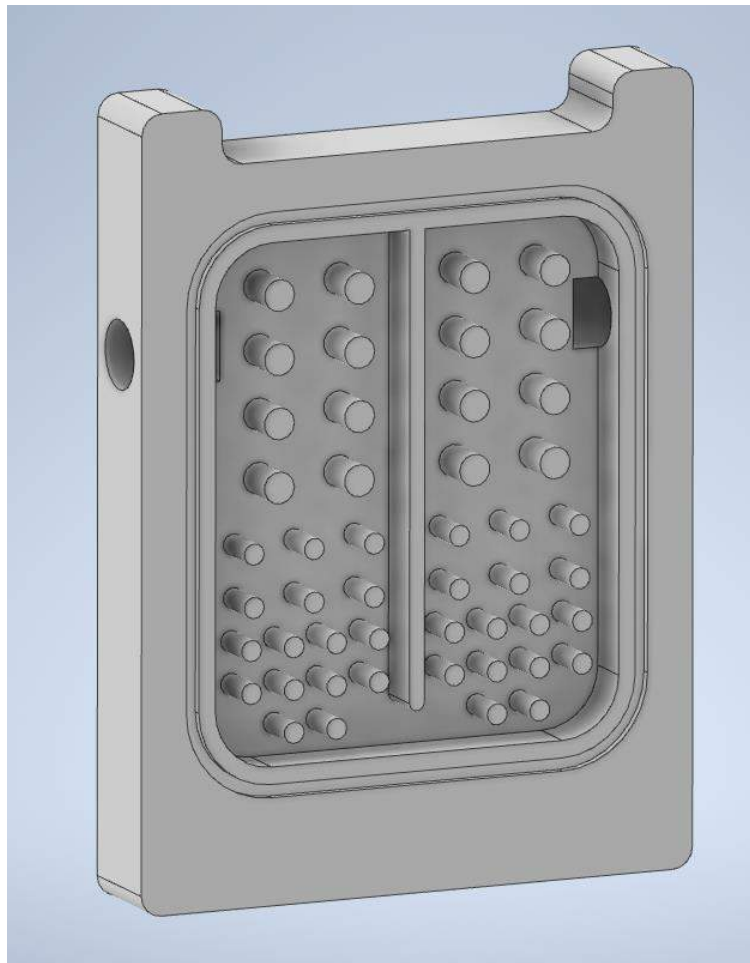


Figure 15: Final pin-fin design.

2.4.4 Module thermal analysis

A preliminary thermal analysis of the entire battery module has been performed. This analysis was done for both a steady state case, and a transient case where the flow direction was switched periodically. In these results the flow was switched every 15 seconds. The boundary conditions used were as follows, an inlet flow rate of 13 ml/s for each cooling block, and outlet pressure of 0 Pa gauge pressure, a heat transfer rate of 6.5 W for each cell dissipated uniformly in the cell volume and all other external surfaces were considered adiabatic. Further analysis of the model will be performed after it has been improved using experimental data.

In the picture below the temperature distribution of the entire module can be observed. Because the ends of the module are considered isolated, the temperature at the ends is considerably higher than in the middle of the module. This observation might, for example, warrant the use of extra cooling blocks on the ends of the module. This decision should be made based on the influence this temperature has on the cells used.

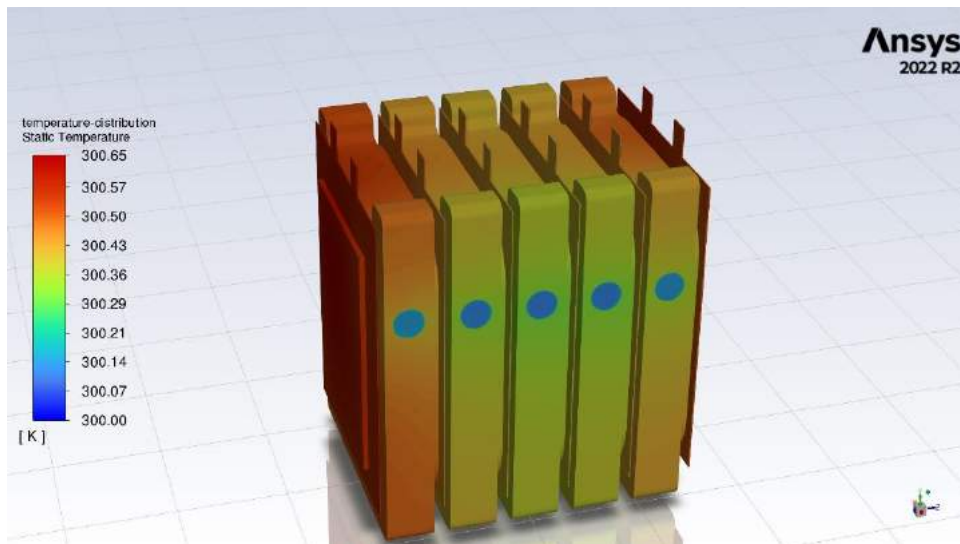


Figure 16: The temperature distribution of the module.

The effects of flow switching was also observed. Underneath the average surface temperature and standard deviation of cell 3 is depicted. Average temperature seemed to rise whilst the standard deviation dropped.

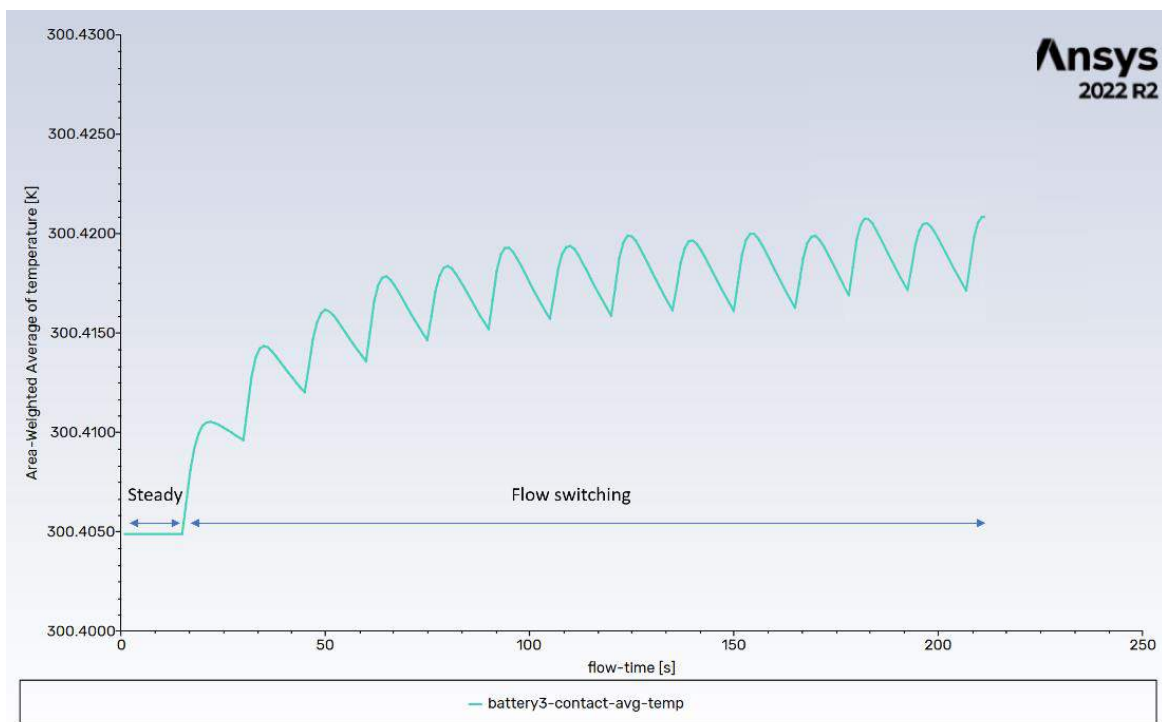


Figure 17: Average temperature comparison - steady VS flow switching.

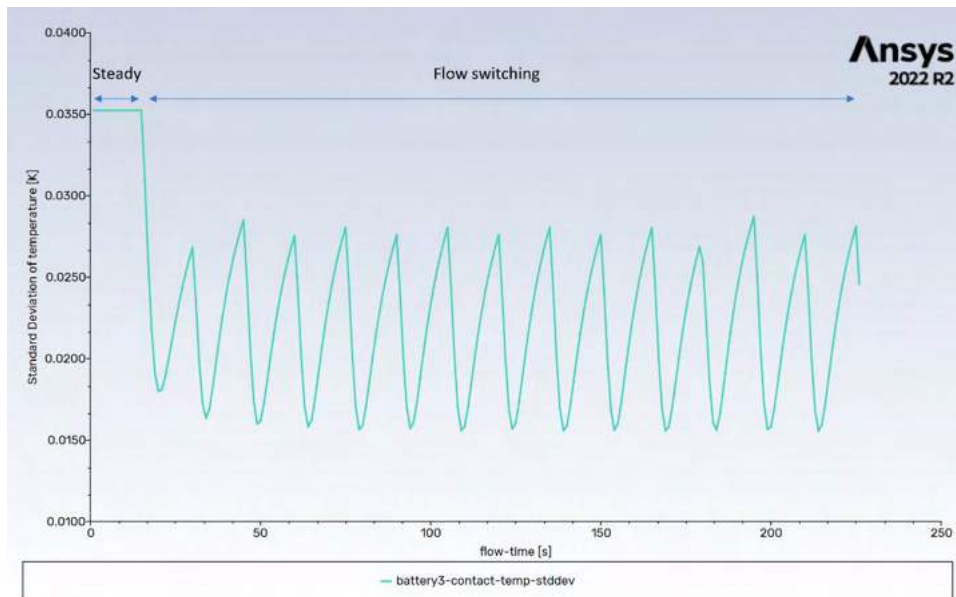


Figure 18: Temperature steady comparison - steady VS flow switching.

The path of the coolant can be visualized by using pathlines. This can aid in designing new cooling solutions by spotting potential problematic areas. Like zones with low coolant flow or recirculation. Many other visualization techniques can be used for this purpose.

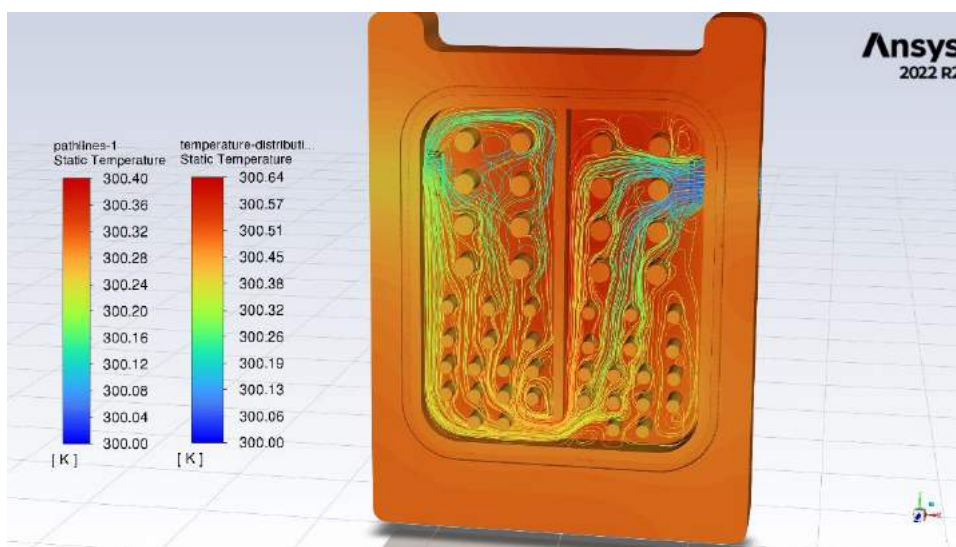


Figure 19: Pathlines and temperature distribution

A more thorough thermal analysis can be performed in future work using the load conditions of the experimental setup used in the SENSIBAT project. These load conditions will be derived from real module measurements and used as input for the simulation. Depending on the results of the simulation the model might need to be adapted to resemble the physical setup more closely, for example by considering convection on the outer walls of the cooling blocks. If the simulation results align with the measurements, it can be used for analysing complex effects that cannot easily be measured on the physical setup.



2.5 PMDU

This section describes briefly the design carried out for the disconnection and monitoring unit of the battery module carried out in the SENSIBAT project by Ikerlan.

2.5.1 Requirements

An attempt has been made to give the design as much flexibility and configurability as possible. In the next table, the specifications defined for the PMDU (Power Measurement and Disconnection Unit) are shown.

Table 4: specifications of the PMDU.

	SPECIFICATION	OBJECTIVE
General Characteristics	Topology	Common path Common or independent path
	Cutting Pole	Negative
	External preload	Sí
	Internal preload	No
	CC protection	Electronic: detection and opening by HW
	OC CHG protection	Electronic: detection by HW and opening by MST
	Fuse	No
	Insulation	No
	Cooling	Coldplate or radiator
Operation Range	Rated Voltage	12V, 24V, 48V
	Voltage Range	0-58.8V
	Discharge current	Configurable (from 10A to 180 ^a)
	Charge current	Configurable (from 10A to 180 ^a)
	Temp. Amb.	-10 a 60°C
Inputs	Enable Discharge	Yes
	Enable Charge	Yes
	Enable Precharge	Yes
	Enable Fan	Yes
	Reset DC protection	Yes
	Power supply +5V	Configurable (3V3 or 5V)
Outputs	Power supply +15V	Yes
	Current measurement	Yes (with high-precision active conditioning)
	Current offset reference	Yes
	Voltage measurement	Yes
	Temp measure radiator	Yes
	Room temp measurement	Yes (NTC input for room temp or other uses)
DC protection statu	Yes (independent on charge and discharge)	



2.5.2. ARCHITECTURE DESIGN

The following figure shows the PMDU seen as a block:

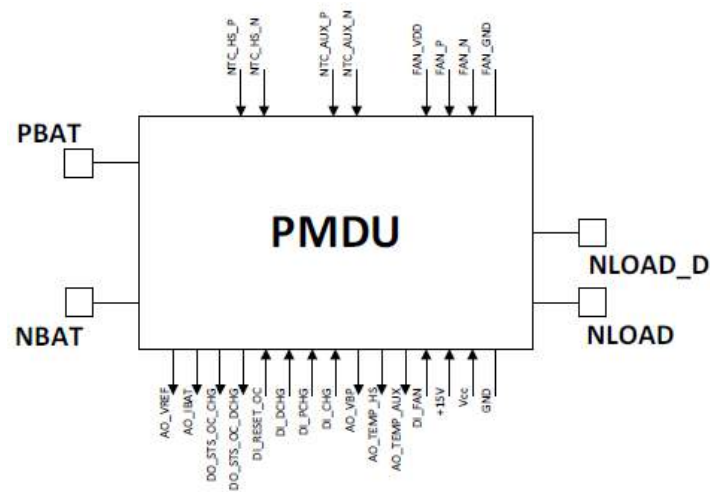


Figure 20: Architecture Design – Main Block.

The figure shows the interfaces, both towards the power part and towards the BMS Master.

Table 5: PMDU interfaces.

POWER INFEACE	
ACRONYM	DESCRIPTION
PBAT	Battery positive pole
NBAT	Battery negative pole
NLOAD	Load negative connection
NLOAD_D	Load negative connection (only discharge)

NTC/FAN INTERFACE	
ACRONYM	DESCRIPTION
NTC_HS_P	Heatsink NTC
NTC_HS_N	Heatsink NTC
NTC_AUX_P	Auxiliary NTC
NTC_AUX_N	Auxiliary NTC
FAN_VDD	External fan supply
FAN_P	Fan positive voltage
FAN_N	Fan negative voltage
FAN_GND	External fan gnd

MASTER INFEACE	
ACRONYM	DESCRIPTION
AO_IBAT	Battery current measurement
AO_VREF	Battery current measurement offset
DO_STS_OC_DCHG	Status overcurrent during discharge
DO_STS_OC_CHG	Status overcurrent during charge
DI_RESET_OC	Reset overcurrent
DI_DCHG	Discharge mosfets command
DI_PCHG	Precharge mosfet command
DI_CHG	Charge mosfet command
AO_TEMP_AUX	Auxiliary temperature measurement
AO_TEMP_HS	Heatsink temperature measurement
DI_FAN	Fan command
AO_VBP	Battery-pack voltage measurement
+15V	+15V supply
Vcc	Vcc supply
GND	Ground

2.5.3 PCB Layout

This design has been mounted on a PCB (Printed Circuit Board) with inlay technology. There are areas in which the PCB consists of the inlay layer, top layer and bottom layer, while in other areas it will be a conventional 4-layer PCB.

The connections to the power part are made on the inlay layer itself and the thicknesses of the respective layers are shown in the next table.



Table 6: specific thicknesses of the respective layers.

	Thickness
Top	70 um
Inlay	2 mm
L1	35 um
L2	35 um
Bottom	70 um

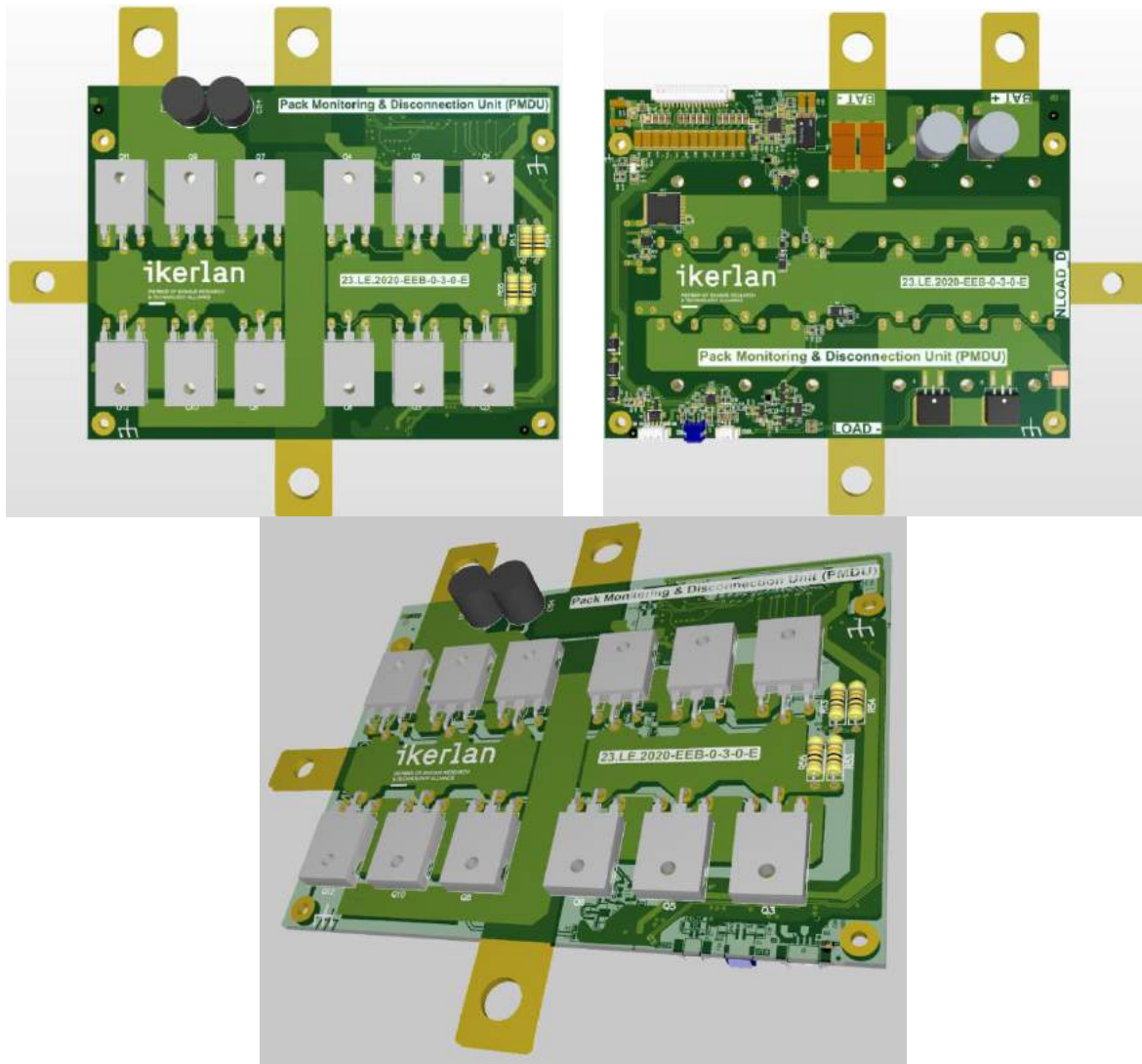


Figure 21: 3D appearance of the assembled PCB.

2.6 BMS Master

This section introduces the BMS Master that will control the SENSIBAT module composed of series connected six 5Ah – L1 cells with sensor matrices for internal pressure and temperature measurements. As a result, the spatial distribution of temperature and pressure over the cell surface are known to the BMS and can be used for advanced state estimation. The BMS collects all the information of each cell provided by the BMS slave and processes it to control the designed junction box.

Figure 22 shows the general architecture of the hardware design, which is composed by a BMS-Master (BMS-M), a Power Measurement and Disconnection Unit (PMDU), a BMS-Slave (SLV) and a PC. On the one hand, the GA No. 957273



BMS-Master is composed by a Raspberry PI 4 model B (RPI) and an Arduino Due (ARD) and on the other hand, the BMS-Slave is based on a transceiver IC (MC33664) and an AFE IC (MC33775A), both from NXP IC. The RPI executes the program code and communicates with ARD and PC or Human-Machine Interface (HMI) while the ARD's function is to interface with the SLV and the PMDU.

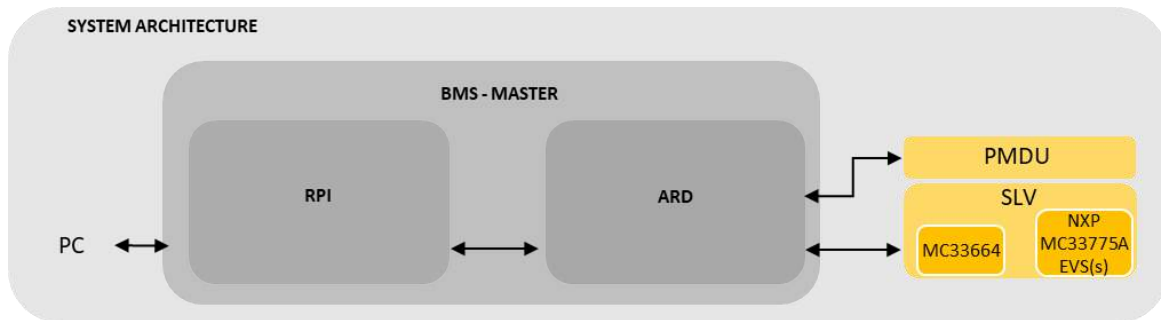


Figure 22: Battery management system architecture (hardware)

The Raspberry PI 4 model B is used to execute the program code containing the improved SoX algorithms and to communicate with a PC or HMI, and an Arduino Due to communicate with the BMS-slave(s) and the PMDU.

Figure 23 shows a photograph of the developed SENSIBAT BMS Master prototype based on a Raspberry PI 4 model B and an Arduino Due.



Figure 23: BMS Master prototype

Figure 24 shows the graphical interface developed in LabVIEW where the most important variables of the battery are available. In addition, Figure 25 shows the 210 internal cell temperature measurements available in the BMS master.

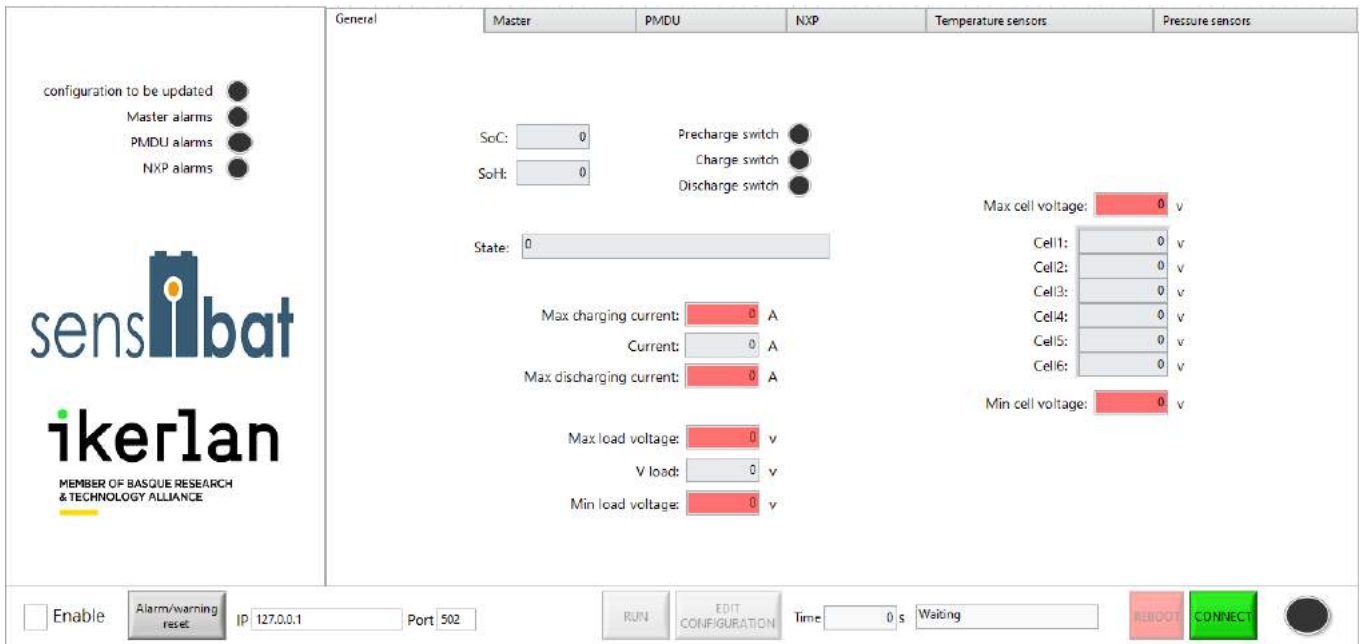


Figure 24: Graphical interface in LabVIEW

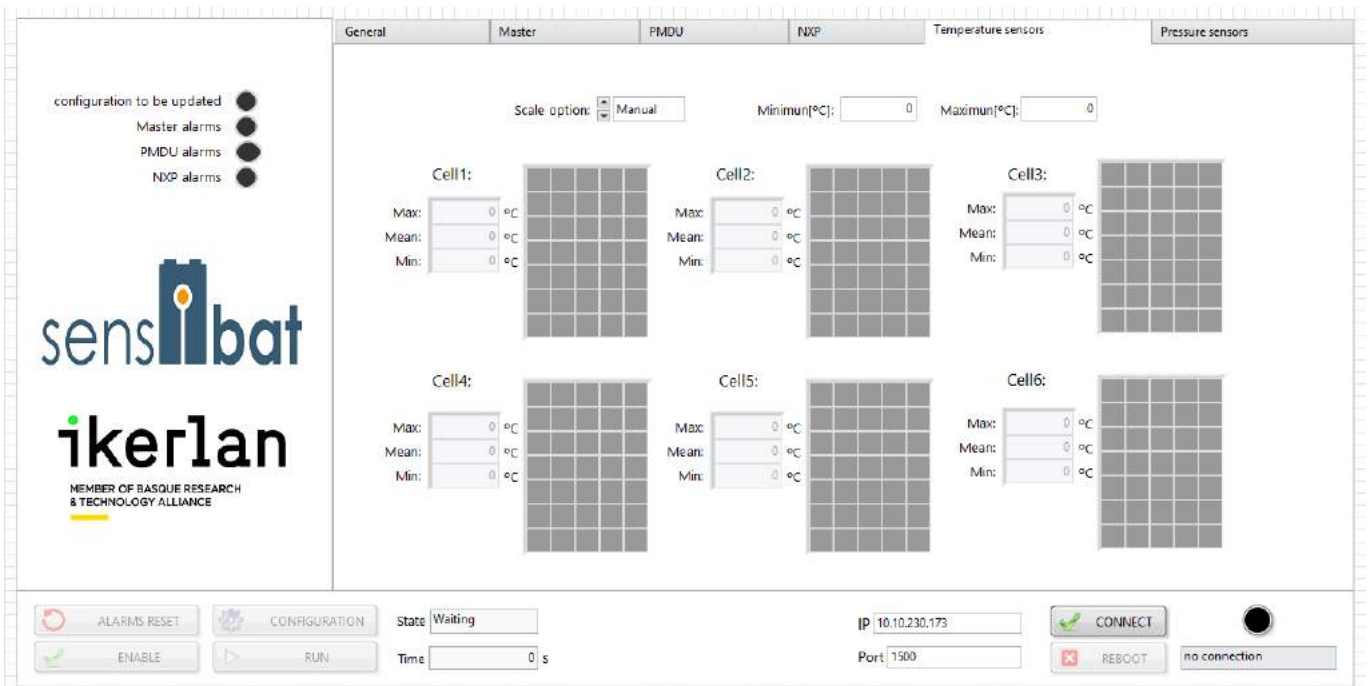


Figure 25: Graphical interface with SENSIBAT module Level 1 sensor data in LabVIEW

The deliverable D4.2 gives more details about the software environment to control a novel BMS-Master design based on a rapid prototyping platform compatible with the advanced BMS slaves presented in the D4.1. This BMS-master allows a reliable and optimal use of the capabilities based on improved accuracy state algorithms (to be developed in Task 4.4).



2.7 BMS Slave

The BMS slave design is based on an AFE developed by NXP (see Figure 26).

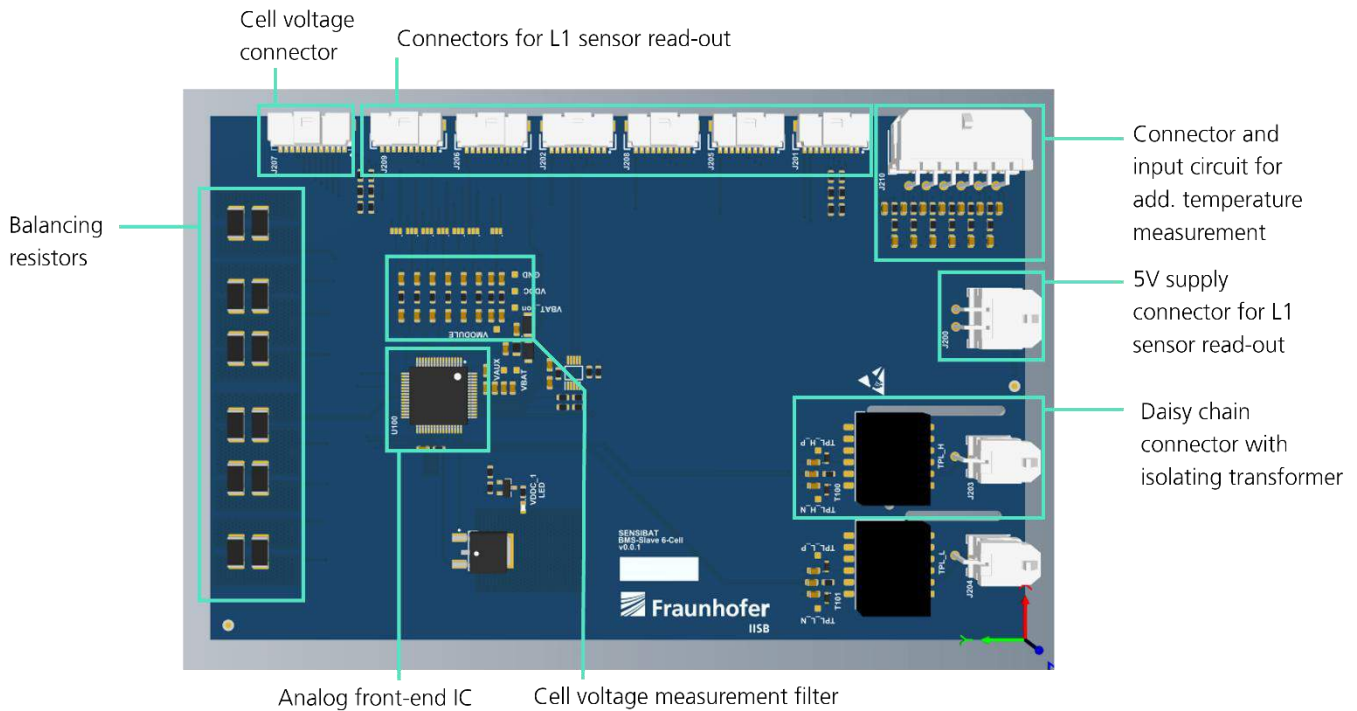


Figure 26: SENSIBAT BMS Slave PCB.

The communication between the BMS slave and the BMS master relies on a proprietary differential daisy chain communication protocol, which is already implemented on the AFE. This ensures high robustness levels against electromagnetic noise, even over longer distances. The BMS slaves are isolated from BMS master by inductively coupling transformers.

The voltages of the six cells of the demonstrator module are directly measured using the voltage sensing inputs of the AFE with passive low pass filtering on every input. Moreover, additional analogue voltage measurements of the AFE are used to read out 6 NTC temperature sensors (one for each cell in the module) to provide a reference for the L1 measurement data. Moreover, the BMS slave provides passive cell balancing controlled by the AFE and using the integrated switches.

The BMS slave is directly powered from the connected cells.

The L1 sensor read out circuits are powered by an external 5V that need to be supplied via connector J200. The communication to the L1 sensor read out circuit uses an I2C interface provided by the AFE. To increase the robustness of the communication, the I2C signals are turned into differential signals using a dedicated interface IC on the BMS slaves and on each read-out circuit.

Every read-out circuit has its own connector, carrying 5V supply and 4 wires of the differential I2C communication.

2.8 Sensor readout module

The sensor readout module has been discussed previously in Deliverable 4.1. For the sake of completeness, a summary of this module is included in this deliverable.



The sensor readout module is a device that reads out both pressure and temperature sensors from the Level 1 sensor cells. There are 5x7 pressure and 5x7 temperature sensors in each cell and the configuration of those sensors make a combined 48 traces that need to be read. Also, the voltages of each cell are read by this PCB. The traces are connected to the readout circuit via a Zero Insertion Force (ZIF) connector. Figure 27 shows the high-level block diagram of the circuit.

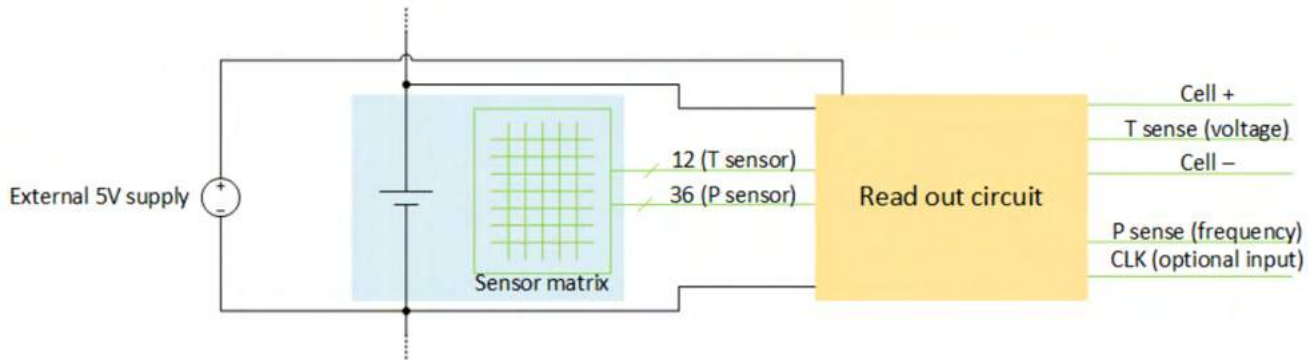


Figure 27: Block diagram of the stand-alone use case scenario of the read-out circuit. Source: D4.1

The PCB can be either controlled autonomously (for stand-alone operation, as shown in Figure 27) or controlled by the BMS-Slave, described in Section 2.7.

Each Level 1 sensor cell is equipped with one sensor readout circuit. Figure 28 shows a photograph of the prototype read-out PCB (50x80mm).



Figure 28: Read-out circuit PCB prototype



3 Discussion & Conclusion

The module, as described in this document houses all technical developments of the SENSIBAT project. It complies to the requirements set out at the start of this task and showcases the various parts of the project in an attractive manner.

The primary functions of the module are the following:

- Validation of the various State Estimation Models: this is ongoing and a conclusion on its effectiveness cannot be made at the time of writing. However, there is no apparent reason why gathering data for validation using the battery module should be problematic.
- Validating the auxiliary hardware: due to issues described in the introduction and the section below this one, the consortium has not been able to validate the BMS master, slave and readout circuits yet.
- Validation of the novel cooling concept: auxiliary sensing hardware will allow us to validate the thermal analysis and subsequent cooling block design.
- Presenting the outcome of the SENSIBAT project in an attractive and convincing display: We believe that the overall design of the SENSIBAT module is reasonably attractive. Special care was taken to have an open design which will allow for easy identification and explanation of all the individual components of the system. The dimensions are suitable for testing and transportation.

As mentioned before, building and testing the full module will result in achieving this important milestone, which we, at the time of writing this document, have not been able to do yet. However, it seems clear to us that the design will achieve the functions described in this chapter. We can guarantee that the chosen cooling hardware will perform well as these have been proven reliable in countless applications and under harsh conditions in other products. The measurement sensors are of industrial grade making these highly reliable.

It is understood that the module design, including the cooling block concept, don't have much industrial relevance, but this was never meant to be the case. Instead, this module has great scientific value to the consortium as it can be an advance cell testing tool, taking advantage of all sensing hardware and cooling options. It is easily adaptable to other cell-types, chemistries and technologies, assuming that the surface area is compatible with the surface area of the cooling blocks. The same is true for the cooling blocks, as new versions can be created and swapped easily, as long as the holes for the threaded rods are on the same locations.

In the interest of modularity and flexibility, all auxiliary hardware and components are mounted to holed plates, making their placement and replacement extremely easy. The holed plates will also help in organizing and guiding the cables that connect all hardware to each other. If the external sensors are not needed for the operation of the module, the top part containing the cell stack and BMS hardware can be easily separated from the bottom cabinet and used in a stand-alone mode. The cooling equipment is contained entirely in the upper module.

3.1 Deviation in the delivery of milestone 5

Milestone 5 is the physical module, built and tested.

The physical construction of the module with all components is underway, with a slight delay related to supply-chain issues on various parts such as the components for the readout-sensor, external sensing hardware and so on.



4 Risks

Risk No.	What is the risk	Probability of risk occurrence ¹	Effect of risk ²	Solutions to overcome the risk
1	Unavailability of components	1	2	There is a list of alternative hardware which we can use in case of unavailability
2	Shipping problems of components	3	1	Extra care will be taken to be sure that the electronics will not be damaged during shipping

¹ Probability risk will occur: 1 = high, 2 = medium, 3 = Low

² Effect when risk occurs: 1 = high, 2 = medium, 3 = Low



5 Acknowledgement

The author(s) would like to thank the partners in the project for their valuable comments on previous drafts and for performing the review.

Project partners

#	PARTICIPANT SHORT NAME	PARTNER ORGANISATION NAME	COUNTRY
1	IKE	IKERLAN S. COOP.	Spain
2	BDM	BEDIMENSIONAL SPA	Italy
3	POL	POLITECNICO DI TORINO	Italy
4	FHG	FRAUNHOFER GESELLSCHAFT ZUR FOERDERUNG DER ANGEWANDTEN FORSCHUNG E.V.	Germany
5	FM	FLANDERS MAKE VZW	Belgium
6	TUE	TECHNISCHE UNIVERSITEIT EINDHOVEN	The Netherlands
7	NXP NL	NXP SEMICONDUCTORS NETHERLANDS BV	The Netherlands
8	NXP FR	NXP SEMICONDUCTORS FRANCE SAS	France
9	ABEE	AVESTA BATTERY & ENERGY ENGINEERING	Belgium
10	VAR	VARTA MICRO INNOVATION GMBH	Germany
11	AIT	AIT AUSTRIAN INSTITUTE OF TECHNOLOGY GMBH	Austria
12	UNR	UNIRESEARCH BV	The Netherlands

DISCLAIMER/ ACKNOWLEDGMENT



Copyright ©, all rights reserved. This document or any part thereof may not be made public or disclosed, copied, or otherwise reproduced or used in any form or by any means, without prior permission in writing from the SENSIBAT Consortium. Neither the SENSIBAT Consortium nor any of its members, their officers, employees or agents shall be liable or responsible, in negligence or otherwise, for any loss, damage or expense whatever sustained by any person as a result of the use, in any manner or form, of any knowledge, information or data contained in this document, or due to any inaccuracy, omission or error therein contained.

All Intellectual Property Rights, know-how and information provided by and/or arising from this document, such as designs, documentation, as well as preparatory material in that regard, is and shall remain the exclusive property of the SENSIBAT Consortium and any of its members or its licensors. Nothing contained in this document shall give, or shall be construed as giving, any right, title, ownership, interest, license, or any other right in or to any IP, know-how and information.

This project has received funding from the European Union's Horizon 2020 research and innovation programme under grant agreement No 957273. The information and views set out in this publication does not necessarily reflect the official opinion of the European Commission. Neither the European Union institutions and bodies nor any person acting on their behalf, may be held responsible for the use which may be made of the information contained therein.